University of South Carolina
Scholar Commons

Faculty Publications | Mechanical Engineering, Department of

3-10-2011

$Sr_2Fe_{1.5}Mo_{0.5}O_6$ as Cathodes for Intermediate-Temperature Solid Oxide Fuel Cells with $La_{0.8}Sr_{0.2}Ga_{0.87}Mg_{0.13}O_3$ Electrolyte

Guoliang Xiao
University of South Carolina - Columbia, xiaogu@engr.sc.edu

Qiang Liu
University of South Carolina - Columbia, qiang@cec.sc.edu

Fei Zhao
University of South Carolina - Columbia

Lei Zhang
University of Science and Technology of China

Changrong Xia
University of Science and Technology of China

Follow this and additional works at: https://scholarcommons.sc.edu/emec_facpub

see next page for additional authors

Part of the Mechanical Engineering Commons

Publication Info

Journal of the Electrochemical Society, Volume 158, Issue 5, 2011, pages B455-B460.
Journal of the Electrochemical Society, Volume 158, Issue 5, 2011, pages B455-B460.
© The Electrochemical Society, Inc. 2011. All rights reserved. Except as provided under U.S. copyright law, this work may not be reproduced, resold, distributed, or modified without the express permission of The Electrochemical Society (ECS). The archival version of this work was published in *Journal of the Electrochemical Society*.
Publisher's Version: http://dx.doi.org/10.1149/1.3556085
PACS: 88.30.pn, 82.47.Ed, 82.80.Fk, 82.45.Rr, 82.45.Gj, 82.45.Fk

This Article is brought to you by the Mechanical Engineering, Department of at Scholar Commons. It has been accepted for inclusion in Faculty Publications by an authorized administrator of Scholar Commons. For more information, please contact digres@mailbox.sc.edu.

Author(s)
Guoliang Xiao, Qiang Liu, Fei Zhao, Lei Zhang, Changrong Xia, and Fanglin Chen

This article is available at Scholar Commons: https://scholarcommons.sc.edu/emec_facpub/16

Journal of The Electrochemical Society, **158** (5) B455-B460 (2011)
0013-4651/2011/158(5)/B455/6/$28.00 © The Electrochemical Society

$Sr_2Fe_{1.5}Mo_{0.5}O_6$ as Cathodes for Intermediate-Temperature Solid Oxide Fuel Cells with $La_{0.8}Sr_{0.2}Ga_{0.87}Mg_{0.13}O_3$ Electrolyte

Guoliang Xiao,[a,*] Qiang Liu,[a,*] Fei Zhao,[a] Lei Zhang,[b] Changrong Xia,[b] and Fanglin Chen[a,*,z]

[a]*Department of Mechanical Engineering, University of South Carolina, Columbia, South Carolina 29208, USA*
[b]*Department of Materials Science and Engineering, University of Science and Technology of China, Hefei, Anhui 230026, China*

The performance of $Sr_2Fe_{1.5}Mo_{0.5}O_6$ (SFMO) as a cathode material has been investigated in this study. The oxygen ionic conductivity of SFMO reaches 0.13 S cm^{-1} at 800°C in air. The chemical diffusion coefficient (D_{chem}) and surface exchange constant (k_{ex}) of SFMO at 750°C are 5.0×10^{-6} cm^2 s^{-1} and 2.8×10^{-5} cm s^{-1}, respectively, suggesting that SFMO may have good electrochemical activity for oxygen reduction. SFMO shows a thermal expansion coefficient (TEC) of 14.5×10^{-6} K^{-1} the temperature range of 200–760°C in air. The polarization resistance of the SFMO cathode is 0.076 Ω cm^2 at 800°C in air under open-circuit conditions measured on symmetrical cells with $La_{0.8}Sr_{0.2}Ga_{0.87}Mg_{0.13}O_3$ (LSGM) electrolytes. Dependence of SFMO cathode polarization resistance on the oxygen partial pressure and the cathode overpotentials at different temperatures are also studied. SFMO shows an exchange current density of 0.186 A cm^{-2} at 800°C in air. Single cells with the configuration of Ni-$La_{0.4}Ce_{0.6}O_2$ (LCO)|LCO|LSGM|SFMO show peak power densities of 349, 468, and 613 mW cm^{-2} at 750, 800, and 850°C, respectively using H_2 as the fuel and ambient air as the oxidant. These results indicate that SFMO is a promising cathode candidate for intermediate-temperature solid oxide fuel cells with LSGM electrolyte.
© 2011 The Electrochemical Society. [DOI: 10.1149/1.3556085] All rights reserved.

Manuscript submitted November 22, 2010; revised manuscript received January 19, 2011. Published March 10, 2011.

Solid oxide fuel cells (SOFCs) have the potential to convert the chemical energy in fuels directly to electricity with fuel flexibility and high efficiency.[1–3] Intermediate temperature SOFCs (IT-SOFCs) operating at 700–800°C are expected to reduce the cost of the SOFC technology while still sustain reasonable fast kinetics for the electrochemical reaction in the electrodes.[4,5] However, it is still challenging for SOFCs to be operated at intermediate temperatures with sufficient power output and durability.

Fuel cell performance greatly depends on the property of the electrolyte materials. When the SOFC operating temperature is lowered, high ionic conductivity is required for the electrolyte materials. The perovskite ionic conductor $La_{0.8}Sr_{0.2}Ga_{0.87}Mg_{0.13}O_3$ (LSGM) has been shown to be an excellent electrolyte candidate for SOFCs operating at intermediate temperatures.[6–8] Besides the electrolyte material, it has also been shown that the cathode material becomes the major obstacle in achieving high cell performance when lowering the cell operating temperature.[9] Generally speaking, the oxygen reduction process at the cathode is mainly responsible for the polarization loss of the fuel cell at intermediate temperatures.[10] The conventional cathode material $La_{1-x}Sr_xMnO_3$ (LSM) is a poor ionic conductor.[11] The active reaction site of oxygen reduction is restricted to the triple phase boundaries (TPBs) at the cathode-electrolyte physical interface. The activation polarization loss of LSM cathode is significant when the cell operating temperature is reduced, making it not suitable as cathode material for IT-SOFCs.

Mixed ionic and electronic conductors (MIECs) are good electrode candidates for SOFCs. MIECs with good electronic and ionic conductivity would promote the oxygen reduction by facilitating the charge transfer process and enlarging the active reaction sites beyond the cathode/electrolyte physical interfaces. Intensive research has been carried out on perovskite oxides based on transition-metal oxides, such as doped $LaFeO_3$, $SrCoO_3$, and La_2NiO_4 (Refs. 10, 12–16). Recently, a novel perovskite $Sr_2Fe_{1.5}Mo_{0.5}O_6$ (SFMO) has been applied as both anode and cathode in symmetrical SOFCs and excellent cell performance has been achieved.[17] SFMO shows high conductivity in both air and hydrogen atmospheres with potential oxygen ion conductivity. SFMO also exhibits good chemical compatibility with LSGM electrolyte. These results suggest that SFMO might potentially be a good cathode candidate with excellent redox stability.

Here we have evaluated SFMO as a cathode with LSGM electrolyte by electrochemical methods. The SFMO cathode sintering temperature and the cathode performance under different oxygen partial pressure have been systematically studied. SFMO has been found to have low over-potential losses at around 800°C, indicating that it can be a very promising cathode candidate for IT-SOFCs based on LSGM electrolyte.

Experimental

Material synthesis and characterization.—SFMO powder was synthesized by a microwave-assisted combustion method. $Sr(NO_3)_2$, $Fe(NO_3)_3$ $9H_2O$ and $(NH_4)_6Mo_7O_{24}$ $4H_2O$ were used as metal precursors. Glycine and citric acid were used to assist combustion. The as-prepared ash was fired at 1000°C for 5 h to form the perovskite structure. The detailed synthesis process can be found elsewhere.[17] $La_{0.8}Sr_{0.2}Ga_{0.87}Mg_{0.13}O_3$ (LSGM) powder was synthesized by solid-state reaction and $La_{0.4}Ce_{0.6}O_2$ (LCO) powder was made by a citric-assisted combustion method.

Characterization.—Phase purities were investigated by a D/MAX-3C x-ray diffractometer with graphite-monochromatized CuKα radiation (λ = 1.5418 Å) before test. The microstructure and morphology of the synthesized product were characterized by scanning electron microscopy (SEM, FEI Quanta 200). The nitrogen adsorption was measured using a Quantachrome Instruments NOVA2000e. The TEC of the SFMO sample sintered at 1400°C was measured by a dilatometer (Netsch DLL 402C/3/G) from room temperature to 1400°C, with an air-purge flow rate of 50 ml min^{-1}. The ionic conductivity of SFMO was measured by a dc method on a cylinder co-pressed with of a thin layer of LSGM as an electronic blocking electrode using the Hebb-Wagner technique.[18] After sintering at 1400°C, the cylinder has a height of 4.2 mm and a diameter of about 5.38 mm. The thickness of the LSGM thin layer is about 150 μm.

The chemical diffusion coefficient (D_{chem}) and surface exchange constant were obtained by the electrical conductivity relaxation (ECR) method. The electrical conductivity was performed by the dc four-probe method on a rectangular bar with relative density of above 95%. After stabilization, the oxygen partial pressure was suddenly changed from 0.21 to 0.1 atm by switching gases and the dependence of the apparent conductivity on time was recorded. The time dependence of the apparent conductivity can be expressed in a rectangular geometry of width $2w$, thickness $2h$ and length $2l$, as[19,20]

* Electrochemical Society Active Member.
z E-mail: chenfa@cec.sc.edu

Downloaded 26 Sep 2011 to 129.252.69.176. Redistribution subject to ECS license or copyright; see http://www.ecsdl.org/terms_use.jsp

$$\frac{\sigma_t - \sigma_0}{\sigma_\infty - \sigma_0} = 1 - \sum_{i=1}^{\infty}\sum_{m=1}^{\infty}\sum_{n=1}^{\infty} \frac{2L_1^2 \exp(-\beta_i^2 D_{\text{chem}} t/h^2)}{\beta_i^2(\beta_i^2 + L_1^2 + L_1)} \times \frac{2L_2^2 \exp(-\gamma_m^2 D_{\text{chem}} t/w^2)}{\gamma_m^2(\gamma_m^2 + L_2^2 + L_2)} \times \frac{2L_1^2 \exp(-\delta_n^2 D_{\text{chem}} t/l^2)}{\delta_n^2(\delta_n^2 + L_3^2 + L_3)} \quad [1]$$

where σ_0, σ_t and σ_∞ denote the initial, time dependent and final conductivities, respectively. The dimensionless parameters L_1, L_2, and L_3 are defined as

$$\frac{D_{\text{chem}}}{k_{\text{ex}}} = \frac{h}{L_1} = \frac{w}{L_2} = \frac{l}{L_3} \quad [2]$$

β_i, γ_m and δ_n are the ith, mth and nth roots of the equations

$$\beta_i \tan \beta_i = L_1 \quad [3a]$$

$$\gamma_m \tan \gamma_m = L_2 \quad [3b]$$

$$\delta_n \tan \delta_n = L_3 \quad [3c]$$

The D_{chem} and k_{ex} can be determined by fitting the relaxation data to Eq. 1.

Cell fabrication and testing.—The LSGM powder was pressed uniaxially at 200 MPa to form pellets and then sintered at 1500°C for 10 h. SFMO, LCO and Ni-LCO (60:40 wt %) powders were mixed with a Heraeus binder V006 (weight ratio of 1:1.5) to form electrode inks.

For symmetrical cells, the SFMO ink was printed on both sides of the LSGM pellets and fired for 1 h at 900, 1000, 1100 and 1200°C, respectively. The LSGM pellet has a diameter of about 13 mm and a thickness of about 0.5 mm. The SFMO electrode has the same diameter of the electrolyte and a thickness of about 25 μm. Pt paste was used as current collectors on the SFMO electrodes. The impedance spectra of the symmetrical cells were measured by a two-electrode configuration under open-circuit conditions. The different oxygen partial pressures were obtained by mixing N_2 with O_2.

The overpotential of SFMO cathode was tested with a three-electrode configuration. LSGM pellets with 15 mm in diameter were used as the electrolyte. The SFMO working electrode (WE) with an area of 0.33 cm^2 was fired on one side of the LSGM pellet at 1000°C for 1 h. A Pt reference electrode (RE) was attached on the same side as the WE, but was 5 mm away from the WE, ensuring that the distance was at least three times the thickness of the electrolyte (about 1 mm). Pt paste was painted symmetrically on the other side of the LSGM pellet as the counter electrode (CE) and it was also used as the current collector for the WE. The cell was fired at 900°C for 1 h before testing. The overpotential was measured by monitoring the current in the cell when a potential step was applied to the WE, and was determined by the following equation

$$\eta_{\text{WE}} = U_{WR} - iR_{\text{el}} \quad [4]$$

Where η_{WE} is the cathode overpotential, U_{WR} is the applied voltage between WE and RE, i is the current flowing through the cell and R_{el} is the resistance of the electrolyte obtained from the impedance spectrum.

The single cell was fabricated on a LSGM pellet with about 300 μm thickness. A layer of LCO was first printed on one side of the LSGM pellet and fired at 1300°C for 1 h. Ni-LCO ink was subsequently printed on LCO interlayer and fired at 1350°C for 2 h. SFMO ink was then printed on the other side of the LSGM pellet and fired at 1000°C for 1 h to form the Ni-LCO LCO LSGM SFMO cells. The SFMO cathode with an area of 0.33 cm^2 was about 25 μm thick after firing. Pt paste was used as current collectors for both electrodes and the cells were tested in a four-probe configuration. H_2 at a flow rate of 40 ml min^{-1} was used as the fuel and ambient air was used as the oxidant.

All the electrochemical characterizations were performed with a Versa STAT 3-400 test system (Princeton Applied Research).

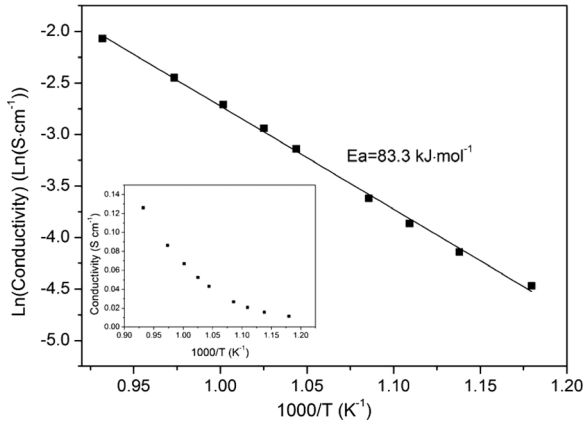

Figure 1. Oxide ionic conductivity of SFMO in air.

Results and Discussion

Ionic conductivity.—MIECs show greater advantages for oxygen reduction as cathode materials than pure electronic conductors, suggesting that the oxide ionic conductivity is also an important parameter for the cathode materials. The oxide ionic conductivity of SFMO at different temperatures in air tested with LSGM as the electronic blocking electrode is shown in Fig. 1. The activation energy calculated from the curve is about 83.3 kJ mol^{-1}. At 800°C in air, the ionic conductivity of SFMO reaches about 0.13 S cm^{-1} which is much higher than that of $La_{0.8}Sr_{0.2}MnO_3$ (5.93×10^{-7} S cm^{-1}) while comparable to that of Co-based cathode materials (0.22 S cm^{-1} for $La_{0.6}Sr_{0.4}CoO_3$, 0.008 S cm^{-1} for $La_{0.6}Sr_{0.4}Co_{0.2}Fe_{0.8}O_3$) (Ref. 21).

D_{chem} and k_{ex}.—Reduction of gaseous oxygen into oxide ions involves both surface exchange and chemical diffusion processes. The bulk diffusion properties and the surface exchange kinetics of a cathode material are closely related to its electrochemical activity for oxygen reduction. These intrinsic properties of the material can be obtained by the electrical conductivity relaxation measurement. Figure 2 shows the time variations of the conductivity of SFMO at 700 and 750°C when the oxygen partial pressure is suddenly

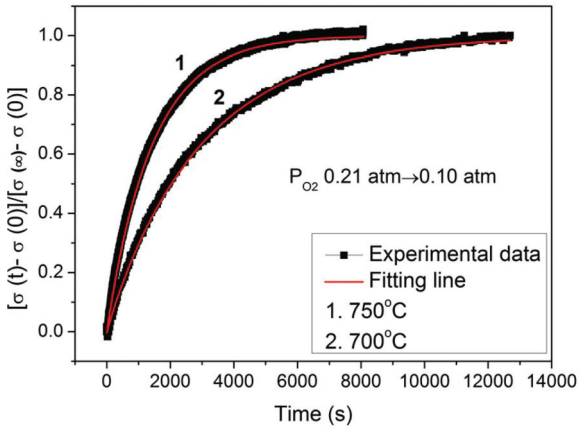

Figure 2. (Color online) Variation of electrical conductivity on time of SFMO after the ambient oxygen partial pressure changed from 0.21 to 0.1 atm.

Downloaded 26 Sep 2011 to 129.252.69.176. Redistribution subject to ECS license or copyright; see http://www.ecsdl.org/terms_use.jsp

Table I. D_{chem} and k_{ex} for SFMO at 700 and 750°C obtained by ECR technique.

Temperature (°C)	D_{chem} ($cm^2\ s^{-1}$)	K_{ex} ($cm\ s^{-1}$)
700	9.0×10^{-7}	1.6×10^{-5}
750	5.0×10^{-6}	2.8×10^{-5}

Table II. The average TECs of SFMO in different temperature ranges in air.

Temperature Range (°C)	TEC ($\times 10^{-6}\ K^{-1}$)
200–760	14.5
760–1200	21.4
200–1200	18.1

changed from 0.21 to 0.1 atm. The D_{chem} and k_{ex} listed in Table I are obtained by fitting these experimental data to the theoretical equations (1)–(3). These values are a bit lower than those reported for $La_{0.6}Sr_{0.4}CoO_3$ (LSC) but comparable to those for $La_{0.6}Sr_{0.4}Co_{0.2}Fe_{0.8}O_3$ (LSCF) under similar conditions,[22,23] suggesting that the SFMO may have similar electrochemical activity for oxygen reduction to that of Co-based cathode materials.

TEC.—Thermal expansion coefficient (TEC) is an important parameter for SOFC cell components. Mismatched TECs of different parts of the cell may lead large internal stress and may result in serious cracks during thermal cycles. The thermal-expansion curve of SFMO from 200 to 1200°C is shown in Fig. 3. A transition in slope at about 760°C can be noticed in the curve, probably due to thermal reduction of SFMO, a phenomenon similar to that of Co-based cathode materials.[20]

The average TECs of SFMO in different temperature ranges are listed in Table II. In the temperature range of 200–1200°C, the TEC of SFMO is about $18.1 \times 10^{-6}\ K^{-1}$ in air, lower than those of the Co-based materials but higher than those of the Mn-based cathodes (e.g., $20.5 \times 10^{-6}\ K^{-1}$ for $La_{0.6}Sr_{0.4}CoO_3$ and $11.8 \times 10^{-6}\ K^{-1}$ for $La_{0.8}Sr_{0.2}MnO_3$ at 800°C in air).[21] However, the TEC of SFMO is much smaller when the temperature is below 760°C, which is about $14.1 \times 10^{-6}\ K^{-1}$ in the temperature range of 200–760°C, indicating that the TEC mismatch for SFMO will be alleviated when the cell is operated under this temperature range.

Sintering temperature.—The electrode fabrication temperature will affect the electrode microstructures, which in turn will have significant influence on the electrode performance, as manifested by the electrode polarization resistance (R_p). Figure 4 shows the interfacial resistances tested at 800°C in air under open-circuit conditions on SFMO symmetrical cells with the electrodes fired for 1 h at 900, 1000, 1100 and 1200°C respectively. Since the intercept of the impedance spectra with the real axis in the high frequency region is related to the total ohmic resistance of the cell and the lead wires, this portion varies a little in each spectrum. The semicircles shown in Fig. 4 are corresponding to the R_p of the cathodes. It can be seen that the R_p of the cell with electrodes fired at 1000°C is the smallest, with a value of only about 0.076 Ω cm^2 at 800°C in air, even lower than that of the LSC cathode on the LSGM electrolyte (~0.089 Ω cm^2 at 800°C in air) (Ref. 24). As shown in Fig. 4, R_p increased when the electrode firing temperature was lowered to 900°C, indicating that the temperature might be too low for SFMO particles to form good connection. On the other hand, R_p increased when the electrodes were fired at 1100°C and it became much larger when the electrode firing temperature was further raised to 1200°C. This is probably due to the decrease in active surface areas in the SFMO cathodes.

Figure 5 shows the cross section views of the symmetrical cells with electrodes fired at different temperatures. As shown in Fig. 5, when the electrode firing temperatures are raised, the average particle size of the SFMO electrode gradually increases. It also reflects that the bonding between particles grows stronger. That may be the reason for the decrease of R_p when the firing temperature increased from 900 to 1000°C. However, the increase in the cathode firing temperature may also decrease the active surface areas of the electrode. According to the nitrogen desorption analysis, the BET surface area of the SFMO powder dropped from around 2 $m^2\ g^{-1}$ to less than 1 $m^2\ g^{-1}$ (decreased more than 50%) after the sintering temperature was raised to 1200°C. This might be the cause of the larger R_p of the SFMO cathodes fired at higher temperatures. The dependences of the polarization resistance of SFMO cathodes on sintering temperatures at different temperatures are shown in Fig. 6. It can be seen that the electrode sintered at 1000°C shows the lowest R_p at nearly all the temperatures tested, indicating that the best sintering temperature for the SFMO cathode is 1000°C.

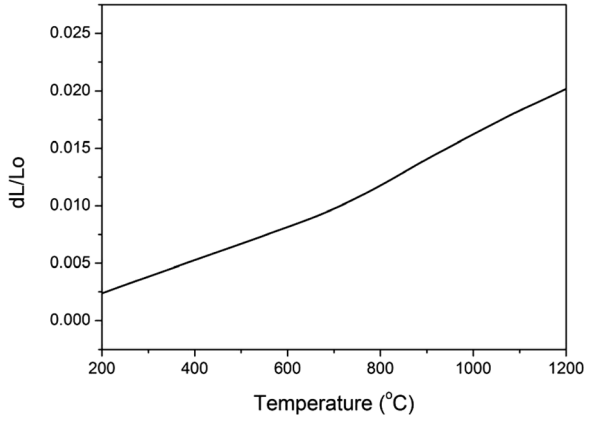

Figure 3. Thermal expansion curve of SFMO measured in air between 200 and 1200°C.

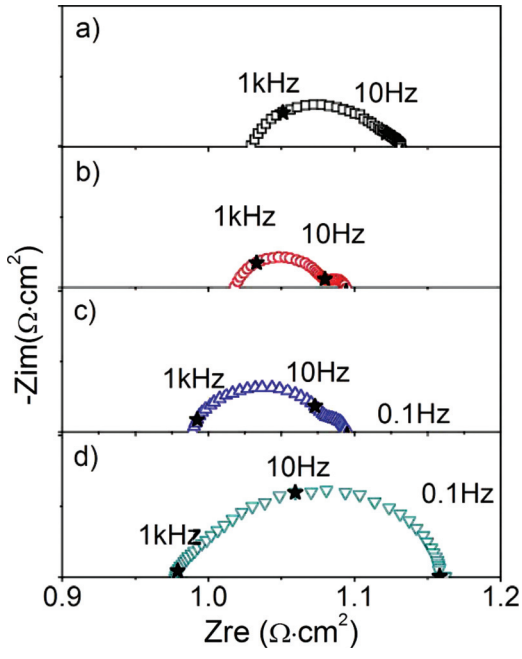

Figure 4. (Color online) Interfacial resistances measured at 800°C in air under open-circuit conditions on SFMO symmetrical cells sintered at (a) 900, (b) 1000, (c) 1100 and (d) 1200°C, respectively. The spectra have been normalized by the electrode areas and a factor of 2 for using symmetrical cells.

Downloaded 26 Sep 2011 to 129.252.69.176. Redistribution subject to ECS license or copyright; see http://www.ecsdl.org/terms_use.jsp

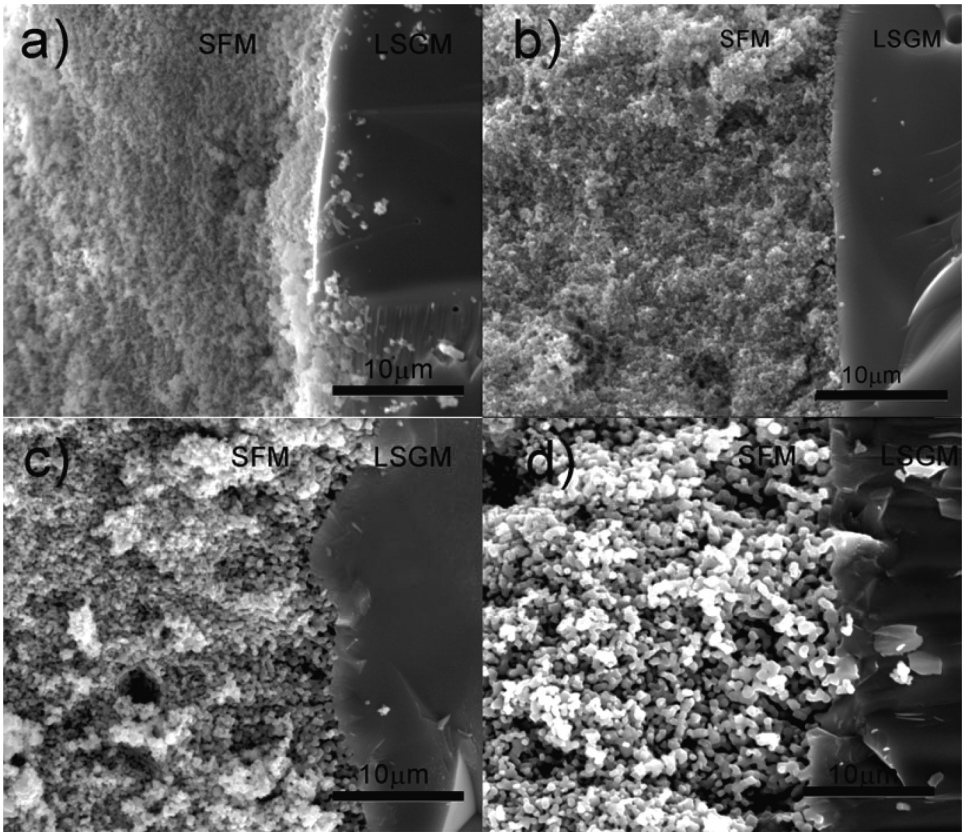

Figure 5. SEM images captured on the cross section of SFMO symmetrical cells sintered at different temperatures: (a) 900°C, (b) 1000°C, (c) 1100°C and (d) 1200°C.

Effect of oxygen partial pressure.—In order to study factors affecting the polarization resistance of SFMO cathode, the impedance spectra of SFMO cathode sintered at 1000°C were recorded under different oxygen partial pressures (Po_2). Figure 7 shows the results at 800°C. As shown in Fig. 7a, at least two arcs can be observed in all obtained impedance spectra, evolving differently with the change of Po_2. In order to study the influence of Po_2 on R_p, an equivalent circuit with a configuration of (R_1CPE_1) (R_2CPE_2) as shown in Fig. 7b was used to fit the two arcs. The fitting results are also shown in Fig. 7a. The dependences of R_1 and R_2 on oxygen partial pressures are shown in Fig. 8. Generally, the relationship between R_p and Po_2 can be represented by the following equation[25,26]

$$R_p = kP_{O2}^{-n} \quad [5]$$

where different values of n may correspond to different reaction steps in the oxygen reduction processes

$$n = 1 : O_{2(g)} \Leftrightarrow O_{2(ads.)} \quad [6]$$

$$n = 1/2 : O_{2(ads.)} \Leftrightarrow 2O_{(ads.)} \quad [7]$$

$$n = 1/4 : O_{(ads.)} + 2e + V_o^{\bullet\bullet} \Leftrightarrow O^{2-} \quad [8]$$

According to Eq. 5, n_1 and n_2 can be obtained by linearly fitting the results of R_1 and R_2, corresponding to 0.36 and 0.97, respectively. These values indicate that the high frequency arc (R_1CPE_1) might be related to the Reaction 8 and the Reaction 7 and the low frequency arc (R_2CPE_2) might be related to the Reaction 6, respectively.

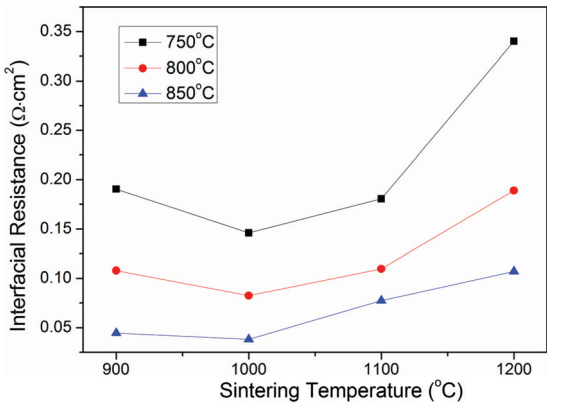

Figure 6. (Color online) Dependence of the interfacial resistance of SFMO electrodes on the sintering temperature at different temperatures.

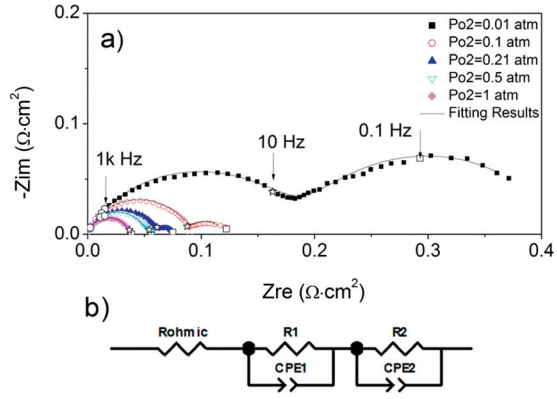

Figure 7. (Color online) (a) Impedance spectra (dots) (normalized by electrode area and factor 2 by symmetrical cells) and fitting results (lines) of the SFMO cathode measured at 800°C under different oxygen partial pressures, (b) equivalent circuit used for fitting.

Downloaded 26 Sep 2011 to 129.252.69.176. Redistribution subject to ECS license or copyright; see http://www.ecsdl.org/terms_use.jsp

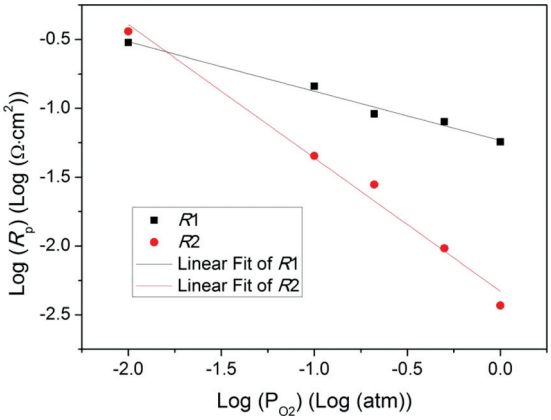

Figure 8. (Color online) Dependence of R_1 and R_2 on oxygen partial pressures at 800°C.

According to the dependence of R_p on Po_2 in Fig. 8, the low frequency arcs in the spectra (with the frequency below 10 Hz) can be related to the oxygen molecule diffusion and adsorption which is sensitively affected by the microstructures of the electrode. It is also found in Fig. 4 that the change in polarization resistance of the electrode fired at different temperatures mainly occurs at the low frequencies and the resistance increases due to the decrease in the active surface areas, consistent with the above discussions.

Cathode overpotential.—SFMO cathode properties under DC polarization were studied by testing the cathode overpotential with a three-electrode configuration. Figure 9 shows the cathode overpotential of SFMO as a function of current density at different temperatures in air.

At low overpotentials, a linear part can be found in each curve which can be expressed by

$$i = \frac{i_0 ZF}{RT}\eta \qquad [9]$$

where i is the current density, i_0 the exchange current density, Z the electron number involved which is 2 for reducing an oxide ion, F the Faraday's constant, R the universal gas constant and η is the cathode overpotential. The exchange current density of SFMO is listed in Table III as well as the values for other conventional cathode materials.[27,28] The exchange current density of SFMO is about 0.18 A cm^{-2} at 800°C in air which is much higher than that of LSM and comparable to those of the Co-based cathode materials. Such good performance of the SFMO cathode is probably due to the relatively high electrical conductivity and ionic conductivity of SFMO.

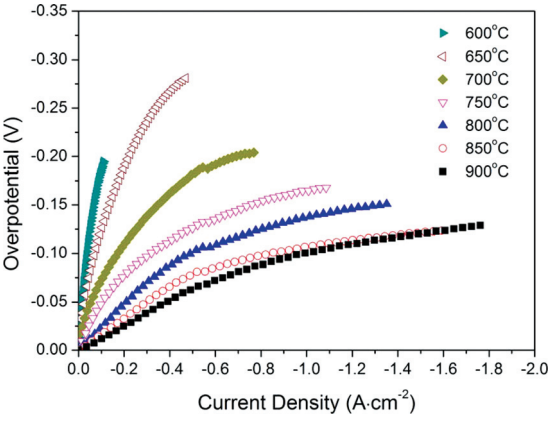

Figure 9. (Color online) Cathode overpotentials measured by a three-electrode configuration at different temperatures in air.

Table III. The exchange current density i_0 (A cm^{-2}) of electrodes at 800°C in air.

Cathode materials	Exchange current density i_0 at 800°C in air (A cm^{-2})
SFMO	0.186
$La_{0.8}Sr_{0.2}MnO_3$	0.003 (Ref. 6), 0.004 (Ref. 25)
$La_{0.6}Sr_{0.4}CoO_3$	0.263 (Ref. 6), 0.519 (Ref. 22), 0.05 (Ref. 25)
$La_{0.6}Sr_{0.4}Co_{0.2}Fe_{0.8}O_3$	0.57 (Ref. 26)

Single cell performance.—The performance of SFMO cathode was tested in LSGM electrolyte supported single cells with Ni-$La_{0.4}Ce_{0.6}O_2$ (LDC) as the anode. According to the previous report,[29] an LDC interlayer was applied between the anode and electrolyte to prevent reactions between LSGM and Ni. The I-V and I-P curves obtained at different temperatures with H_2 as the fuel and ambient air as the oxidant are shown in Fig. 10. It can be seen that the maximum power densities are 349, 468, and 613 mW cm^{-2} at 750, 800, and 850°C, respectively. The impedance spectra of the single cell obtained under open-circuit conditions at different temperatures are shown in Fig. 11. The polarization resistance of the whole cell is 0.32 Ω cm^{-2} at 800°C, much larger than that of the SFMO cathode measured in symmetrical cells under open-circuit conditions (0.076 Ω cm^2), indicating that the anode performance limits the cell power output. Consequently, the cell performance is expected to be further improved by optimizing the anode to reduce the anode polarization losses. Additionally, SFMO shows reduction and oxidation (redox) stability and compatibility with the LSGM electrolyte as reported elsewhere.[17] These results suggest that SFMO is a very promising cathode candidate for IT-SOFCs with LSGM electrolyte.

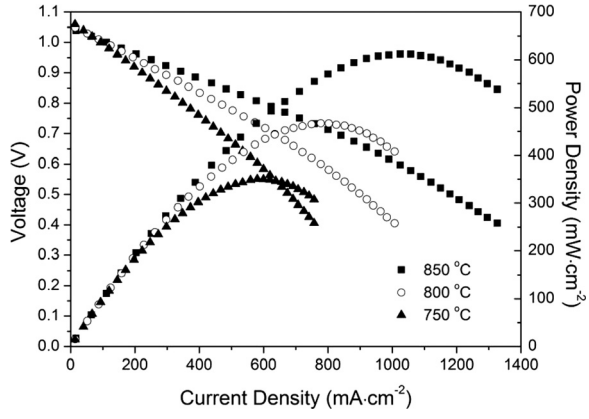

Figure 10. Performance of the single cell (Ni-LCO LCO LSGM SFMO) with H_2 as the fuel and ambient air as the oxidant at different temperatures.

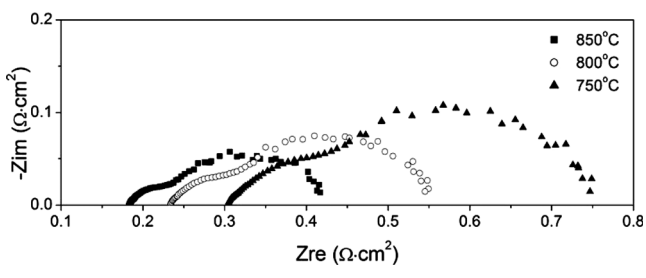

Figure 11. Impedance spectra of the single cell (Ni-LCO LCO LSGM SFMO) measured under open-circuit conditions at different temperatures.

Downloaded 26 Sep 2011 to 129.252.69.176. Redistribution subject to ECS license or copyright; see http://www.ecsdl.org/terms_use.jsp

Conclusions

Perovskite oxide SFMO shows high oxide ionic conductivity of 0.13 S cm^{-1} at 800°C. The D_{chem} and k_{ex} measured on SFMO by the electrical relaxation method are comparable to those of LSC while the TEC is even lower. The SFMO cathode sintered at 1000°C for 1 h shows the lowest polarization resistance. The polarization resistance of the SFMO cathode is 0.076 Ω cm^2 at 800°C in air under open-circuit conditions measured on symmetrical cells with LSGM electrolytes. In addition, SFMO shows an exchange current density of 0.186 A cm^{-2} at 800°C in air. Single cells with the configuration of Ni-LCO|LCO|LSGM|SFMO show peak power densities of 468 mW cm^{-2} at 800 using H_2 as the fuel and ambient air as the oxidant. These results indicate that SFMO is a promising cathode candidate for intermediate-temperature solid oxide fuel cells with LSGM electrolyte.

Acknowledgment

G.L.X., Q.L., F.Z., and F.L.C. gratefully acknowledge the financial support from the Department of Energy (Award Number DE-SC0001061) and NASA EPSCoR (Award Number NNX10AN33A). C.R.X. and L.Z. would like to thank the financial support from Natural Science Foundation of China (50730002).

University of South Carolina assisted in meeting the publication costs of this article.

References

1. D. J. L. Brett, A. Atkinson, N. P. Brandon, and S. J. Skinner, *Chem. Soc. Rev.*, **37**, 1568 (2008).
2. R. M. Ormerod, *Chem. Soc. Rev.*, **32**, 17 (2003).
3. M. D. Gross, J. M. Vohs, and R. J. Gorte, *J. Mater. Chem.*, **17**, 3071 (2007).
4. A. Orera and P. R. Slater, *Chem. Mater.*, **22**, 675 (2010).
5. S. D. Park, J. M. Vohs, and R. J. Gorte, *Nature (London)*, **404**, 265 (2000).
6. K. Q. Huang, M. Feng, J. B. Goodenough, and C. Milliken, *J. Electrochem. Soc.*, **144**, 3620 (1997).
7. K. Q. Huang, P. Y. Hou, and J. B. Goodenough, *Solid State Ionics*, **129**, 237 (2000).
8. K. Q. Huang, J. H. Wan, and J. B. Goodenough, *J. Electrochem. Soc.*, **148**, A788 (2001).
9. Z. P. Shao and S. M. Haile, *Nature (London)*, **431**, 170 (2004).
10. S.-E. Hou, J. A. Alonso, S. Rajasekhara, M. J. Martinez-Lope, M. T. Fernandez-Diaz, and J. B. Goodenough, *Chem. Mater.*, **22**, 1071 (2010).
11. A. Hammouche, E. J. L. Schouler, and M. Henault, *Solid State Ionics*, **28–30**, 1205 (1988).
12. J. J. Cheng, A. Navrotsky, X. D. Zhou, and H. U. Anderson, *Chem. Mater.*, **17**, 2197 (2005).
13. H. Kishimoto, N. Sakai, T. Horita, K. Yamaji, M. E. Brito, and H. Yokokawa, *Solid State Ionics*, **178**, 1317 (2007).
14. V. V. Vashook, N. E. Trofimenko, H. Ullmann, and L. V. Makhnach, *Solid State Ionics*, **131**, 329 (2000).
15. A. Aguadero, J. A. Alonso, D. Perez-Coll, C. D. L. Calle, M. T. Fernandez-Diaz, and J. B. Goodenough, *Chem. Mater.*, **22**, 789 (2010).
16. M. Bevilacqua, T. Montini, C. Tavagnacco, E. Fonda, P. Fornasiero, and M. Graziani, *Chem. Mater.*, **19**, 5926 (2007).
17. Q. Liu, X. H. Dong, G. L. Xiao, F. Zhao, and F. L. Chen, *Adv. Mater.*, **22**, 5478 (2010).
18. I. Riess, *Solid State Ionics*, **91**, 221 (1996).
19. I. Yasuda and M. Hishinuma, *J. Solid State Chem.*, **123**, 382 (1996).
20. C. Huang, D. Chen, Y. Lin, R. Ran, and Z. Shao, *J. Power Sources*, **195**, 5176 (2010).
21. C. Sun, R. Hui, and J. Roller, *J. Solid State Electrochem.*, **14**, 1125 (2010).
22. W. Sitte, E. Bucher, and W. Preis, *Solid State Ionics*, **154–155,** 517 (2002).
23. M. Sahibzada, W. Morton, A. Hartley, D. Mantzavinos, and I. S. Metcalfe, *Solid State Ionics*, **136–137**, 991 (2000).
24. T. Horita, K. Yamaji, N. Sakai, H. Yokokawa, A. Weber, and E. Ivers-Tiffee, *J. Electrochem. Soc.*, **148**, A456 (2001).
25. Q. Li, Y. Fan, H. Zhao, L. P. Sun, and L. H. Huo, *J. Power Sources*, **167**, 64 (2007).
26. E. Siebert, A. Hammouche, and M. Kleitz, *Electrochim. Acta*, **40**, 1741 (1995).
27. F. Lecarpentier, H. L. Tuller, and N. Long, *J. Electroceram.*, **5**, 225 (2000).
28. A. Esquirol, N. Bonanos, N. P. Brandon, J. Kilner, and M. Mogensen, *J. Electrochem. Soc.*, **151**, A1847 (2004).
29. K. Q. Huang, R. Tichy, J. B. Goodenough, and C. Milliken, *J. Am. Ceram. Soc.*, **81**, 2581 (1998).

Downloaded 26 Sep 2011 to 129.252.69.176. Redistribution subject to ECS license or copyright; see http://www.ecsdl.org/terms_use.jsp